

## Temperature effect on the performance of phthalocyanine based photovoltaic devices

Hemant Kumar<sup>a,b</sup>, Pankaj Kumar<sup>a\*</sup>, Neeraj Chaudhary<sup>a</sup>, Ramil Bhardwaj<sup>a</sup>, G D Sharma<sup>a</sup>,  
P Venkatesu<sup>b</sup> & Suresh Chand<sup>a</sup>

<sup>a</sup>Centre for Organic Electronics, National Physical Laboratory (CSIR), Dr K S Krishnan Road, New Delhi 110 012, India

<sup>b</sup>Department of Chemistry, University of Delhi, Delhi 110 007, India

Received 25 November 2009; accepted 5 August 2010

In this paper, the effect of temperature on performance of phthalocyanine based photovoltaic devices is investigated. Zinc phthalocyanine (ZnPc) and metal free phthalocyanine (H<sub>2</sub>Pc) are used as donor whereas fullerene (C<sub>60</sub>) is used as an acceptor. Prior to these investigations, the thicknesses of the active layers are optimized to get the optimum performance. The optimised device has an efficiency of ~1.4% for ZnPc and ~0.5% for H<sub>2</sub>Pc at room temperature. Investigations on the optimized device show that temperature has significant effect on the photovoltaic performance. Short circuit current density ( $J_{sc}$ ) and fill factor ( $FF$ ) decrease whereas open circuit voltage ( $V_{oc}$ ) increases with reduction in temperature. The reduction in  $J_{sc}$  has been attributed to the temperature dependent electronic properties of the active organic layers while the increment in the  $V_{oc}$  has been attributed to the reduction in band bending and increment in built in voltage ( $V_{bi}$ ) on lowering of temperature. In overall the efficiency first increases and then decreases with reduction in temperature.

**Keywords:** Organic photovoltaic, Phthalocyanine, Electronic properties, Fill factor, Short circuit current density, Open circuit voltage

In the last two decades a new branch of photovoltaic research, known as organic photovoltaic (OPV) has evolved which is now considered to be an alternate to conventional inorganic solar cells. OPV devices are considered to be the most promising alternative sources of energy as they can play an important role in generating cost effective long term and clean energy along with other potential features, such as light weight, flexibility, and ease in fabrication of large area devices. These technological potentials are now driving the attention of researchers towards further improvement in the performance of these devices. The performance of OPV devices has improved a lot in the last decade through various device designs, different physical treatments and variation of materials and processing techniques. Power conversion efficiency ( $\eta$ ) of ~ 6.5 % has been achieved in tandem OPV devices based on polymer:fullerene bulk heterojunctions<sup>1</sup>. Stability and reliability are the major concerns for these devices and lots of research is being done in this area as well. Because of continuous efforts and hard work of the researchers, several thousand hours life time of OPV

devices has been achieved<sup>2-4</sup>. The power conversion efficiency of a solar cell depends on  $V_{oc}$ ,  $J_{sc}$  and  $FF$  as

$$\eta = \frac{J_{sc} V_{oc} FF}{P_{in}} \quad \dots (1)$$

where  $P_{in}$  is the incident optical power. Under light illumination the absorbed light photons generate excitons, which diffuse to the donor acceptor interface and dissociate there. The efficient dissociation of photo-generated excitons and rapid transportation of the separated charge carriers through the active layers leads to the high efficiency in these devices.

Depending upon the materials to be used, the OPV devices can be prepared either by spin coating or by thermal evaporation of the materials in vacuum. For reliability of these devices in different environmental conditions it becomes very important to investigate the effect of various physical parameters, e.g., temperature, humidity, electric field, magnetic field and illumination intensity on their performance. In this paper, the effect of temperature on the performance of OPV devices based on thermally evaporated phthalocyanines has been investigated. For this purpose two important phthalocyanines, viz., ZnPc and H<sub>2</sub>Pc were used along with C<sub>60</sub>. First of all

\*Corresponding author (E-mail: pankaj@mail.nplindia.ernet.in)

the thicknesses of active layers were optimized to get the best efficiency with these systems. The effect of temperature on the performance of indium tin oxide (ITO) / phthalocyanine/ $C_{60}$ /bathophenanthroline (BPhen)/Al OPV devices has been investigated. These studies have been carried out both in dark as well as under light illumination. The interesting results along with their interpretations have been discussed. This research throws adequate light on elucidating the mechanism governing the charge carrier transport and generation of photocurrent/photo-voltage in the OPV devices as a function of working temperature.

### Experimental Procedure

The devices were prepared on the pre-patterned and pre-cleaned ITO substrates in ITO/phthalocyanine/ $C_{60}$ /BPhen/Al configuration, where BPhen works as exciton blocking layer. Application of exciton blocking layer reduces the exciton quenching at cathode and improves the cell performance<sup>5</sup>. Figure 1 shows the molecular structures of the materials and schematic structure of the device. Prior to any deposition the ITO substrates were exposed to air plasma for 5 min and then transferred to a vacuum chamber, where thin film depositions were carried out via thermal evaporation of the materials at the base pressure  $\sim 5 \times 10^{-6}$  Torr.

All the materials were obtained from Sigma-Aldrich USA and were used as such. To eliminate the performance variance due to fabrication conditions, the devices were fabricated in a controlled way under identical conditions. The rate of evaporation of these materials was monitored with a oscillating quartz crystal and maintained between 0.1-0.4 Å/s. Al

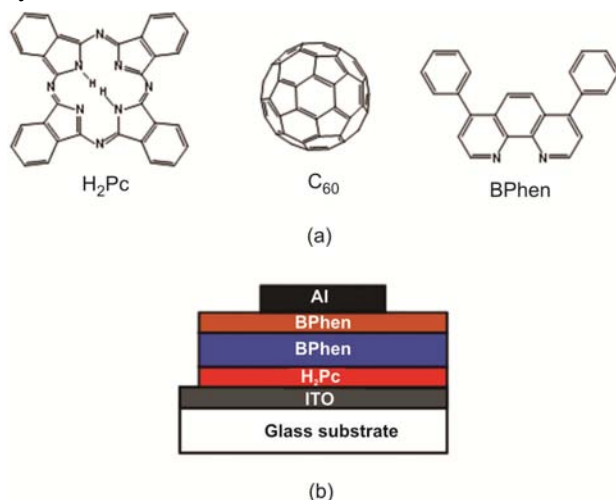


Fig. 1– Molecular structures of the materials used with schematic structural diagram of the  $H_2Pc/C_{60}$  solar cell

cathodes were deposited through the shadow masks. For low temperature measurements the device was transferred to a laboratory made low temperature measurement assembly, where the current density-voltage ( $J$ - $V$ ) characteristics were carried out in dark and under halogen lamp illumination with irradiance of  $80 \text{ mW/cm}^2$ . A Keithley 2400 Source-Measure unit, interfaced with a computer, was used to measure the  $J$ - $V$  characteristics.

### Results and Discussion

The power conversion efficiency of an OPV device depends upon the absorption efficiency, exciton dissociation efficiency, transport of charge carriers and charge collection efficiency. Absorption of incident photons and exciton dissociation are decided by the thickness of the photoactive layers. The best performance can only be achieved by the optimisation of various parameters. For the same objective we varied the thicknesses of phthalocyanines and  $C_{60}$  in the configuration ITO/phthalocyanine ( $x \text{ nm}$ )/ $C_{60}$  ( $y \text{ nm}$ )/BPhen (8 nm)/Al (150 nm), where  $x$  and  $y$  have been varied. To optimize the thickness of ZnPc, first of all  $y$  was kept at 40 nm and  $x$  was varied from 20 to 27 nm. For  $x = 20 \text{ nm}$  the device exhibited a short circuit current ( $J_{sc}$ ) =  $2.5 \text{ mA/cm}^2$ , open circuit voltage ( $V_{oc}$ ) = 0.58 V, fill factor ( $FF$ ) = 19% and  $\eta = 0.33 \%$ . When the thickness of ZnPc was increased to 22 nm both the  $J_{sc}$  and  $FF$  were observed to increase but  $V_{oc}$  decreased. The increment in the product of  $J_{sc}$  and  $FF$  overcame to the reduction in  $V_{oc}$  and the overall efficiency was observed to increase. The increment in  $J_{sc}$  can be attributed to the enhanced absorption of incident light in ZnPc due to increased thickness resulting large photo-current. The reason behind the reduction in  $V_{oc}$  has to be well understood. A further increment in  $x$  from 20 to 25 nm resulted into  $\sim 84 \%$  increment in  $J_{sc}$ ,  $\sim 2$  times increment in  $FF$  and  $\sim 3$  times increment in  $\eta$  (1.38 %). This increment can again be attributed to the enhanced absorption of incident light in ZnPc due to increased thickness resulting large photo-current and efficiency. When the thickness of ZnPc was increased beyond 25 nm both the  $J_{sc}$  and  $FF$  were observed to decrease which resulted into the reduction in  $\eta$ . This reduction in the performance of the device can be attributed to the increased series resistance introduced by the additional thickness of ZnPc. Therefore, the optimum thickness of ZnPc was observed to be 25 nm. Once the thickness of ZnPc was optimized it was kept at 25 nm for rest of the devices and  $C_{60}$  was varied from

35 to 43 nm. The similar interpretation as used for ZnPc can be used to explain the parameter variance of the OPV devices due to variation in the thickness of  $C_{60}$ . The optimum thickness of  $C_{60}$  was found to be 37 nm for which the device exhibited the maximum efficiency of 1.38%. Similarly the optimum thickness of  $H_2Pc$  and  $C_{60}$  were found to be 23 and 40 nm respectively and the cell exhibited  $V_{oc} = 0.43$  V,  $FF = 40\%$ ,  $J_{sc} = 2.3$  mA/cm<sup>2</sup> and an efficiency of 0.53%. The variation of  $V_{oc}$  with active layer thickness is interesting because in the literature  $V_{oc}$  has been correlated with the difference ( $I_g$ ) between the lowest unoccupied molecular orbital (LUMO) of acceptor and highest occupied molecular orbital (HOMO) of the donor material at the heterojunction interface<sup>6,7</sup>, and with the difference of work functions of the electrodes used<sup>8</sup>. In the present studies neither the materials nor the electrodes have been changed, still a change in  $V_{oc}$  has been observed just because of thickness variation. The change in  $V_{oc}$  on the variation of active layer thickness has also been observed in boron subphthalocyanine chloride (sub-Pc)/ $C_{60}$  OPV devices reported earlier<sup>9</sup> but the reason is not well understood. So these types of observations open the new doors for further research in the area of OPV devices.

Once the devices were optimized, the effect of temperature on their performance was studied. Figure 2 shows the dark  $J$ - $V$  characteristics of ZnPc based optimized device on semi-log scale, measured at different temperatures in the range 299-120 K. The dark current is determined by the charge carriers

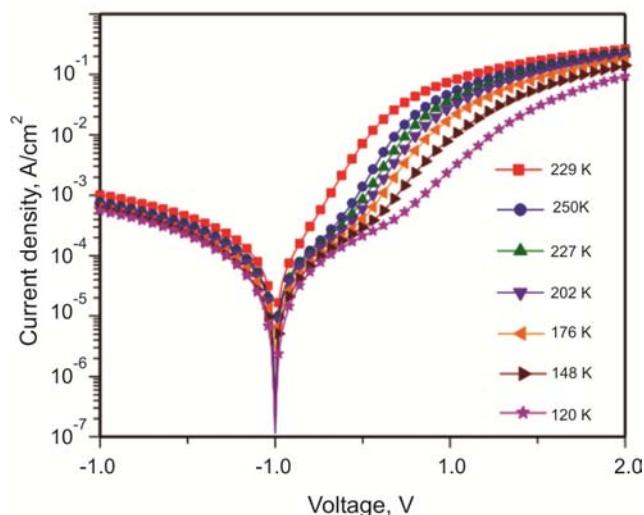


Fig. 2— $J$ - $V$  characteristics of ITO/ZnPc(25 nm)/ $C_{60}$  (37 nm)/Bphen (8 nm)/Al OPV device measured in dark at different temperatures in the range 299-120 K

injected through the electrodes and is observed to decrease with reduction in temperature. At low temperatures the reduction in reverse bias current is relatively low compared to that in the forward bias (+ve voltage to ITO) current. The reduction in dark current with reduction of temperature can be explained by the temperature dependent charge transport properties of the active organic layers. In the reverse bias (+ve voltage to Al) below 227 K the current became almost temperature independent. Temperature independency of the current below 221 K in the reverse bias suggests that the current might be controlled the tunnelling of the charge carriers through large injection barriers<sup>10</sup>. The current shows ohmic behaviour at 299 K in the reverse bias. This ohmic behaviour in the reverse bias can probably be attributed to the high charge injection barriers in the reverse bias<sup>11-13</sup>.

At low temperatures charges do not have sufficient energy to overcome the injection barriers and therefore are injected into the semiconductor via tunnelling through the barriers. The OPV device based on  $H_2Pc$  also exhibited the same behaviour. It is thus established that the reverse bias current in the present OPV devices is governed by tunnelling mechanism at low temperatures.

Figure 3 shows the illuminated  $J$ - $V$  characteristics of ZnPc based OPV device at different temperatures on a semi-log scale, whereas the inset shows the  $J$ - $V$  characteristics of that based on  $H_2Pc$ . The temperature exhibited significant effect on the current under

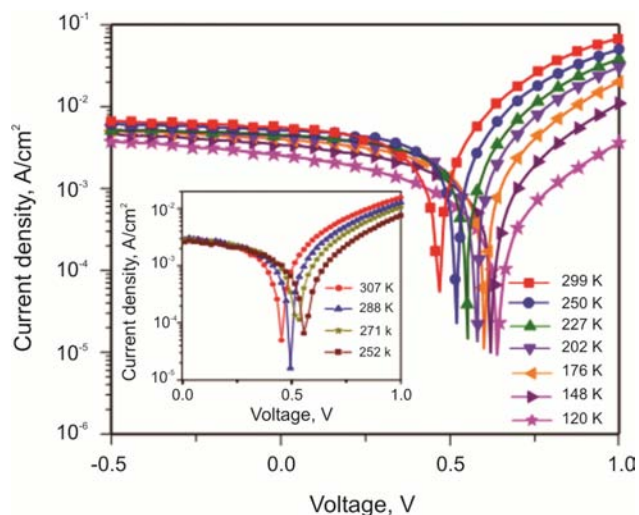


Fig. 3— $J$ - $V$  characteristics of ITO/ZnPc(25 nm)/ $C_{60}$  (37 nm)/Bphen (8 nm)/Al OPV device under 80 mW/cm<sup>2</sup> irradiance of halogen lamp at different temperatures. Inset shows the illuminated  $J$ - $V$  characteristics ITO/ $H_2Pc$ (23 nm)/ $C_{60}$ (40 nm)/Bphen(8 nm)/Al solar cell at different temperatures

illumination as well. The current is observed to decrease with reduction in temperature. Figure 4 shows the effect of temperature on  $J_{sc}$  and  $V_{oc}$  of the H<sub>2</sub>Pc based devices. The device based on ZnPc exhibited a similar performance (not shown). It is observed that the  $J_{sc}$  decreases while  $V_{oc}$  increases with reduction in temperature. Organic semi-conductors are generally amorphous in nature and contain traps. The temperature dependence of  $J_{sc}$  can be attributed to the electronic transport properties of the active organic materials. Their charge carrier mobilities are very low and depend on the temperature. Furthermore, it is negatively influenced by the capture of charge carriers by traps. One would expect that the lowering of temperature will reduce the current<sup>14</sup>. Therefore, reduction in  $J_{sc}$  can be interpreted in terms of trapping effect and the reduction of charge carrier mobility with temperature.

Regarding the variation of  $V_{oc}$  with temperature, the origin of  $V_{oc}$  itself is not well understood. Different models have been presented to explain the experimental observations<sup>7,15</sup>. However, the temperature variation of  $V_{oc}$  could not directly be explained by these models. The temperature dependence of  $V_{oc}$  in the present case makes it further difficult to explain the explicitly origin of  $V_{oc}$ . In conventional Si solar cells the temperature dependence of  $V_{oc}$  is given by

$$V_{oc} = \frac{nkT}{q} \ln \left( \frac{J_{sc}}{J_0} + 1 \right) \quad \dots (2)$$

where  $J_0$  is the reverse saturation current in the device and  $n$  is the diode ideality factor. Here both the  $J_{sc}$  and  $J_0$  also depend on temperature and increase with increase in temperature<sup>16,17</sup>. Though increase in  $J_{sc}$  would slightly increase  $V_{oc}$  but due to large increase in  $J_0$  ( $J_0$  is proportional to  $n_i^2$ , where  $n_i$  is intrinsic charge

carrier density) would rapidly decrease  $V_{oc}$  with increment in temperature<sup>16</sup>. Katz *et al.*<sup>16</sup> investigated the effect of temperature on  $J_{sc}$ ,  $V_{oc}$ ,  $FF$  and  $\eta$  in a poly(2-methoxy, 5-(3,7 dimethyl-octyloxy))-*p*-phenylene-vinylene (MDMO-PPV): [6,6] phenyl C<sub>61</sub>-butyric methyl-ester (PCBM) based bulk-heterojunction OPV device in the temperature range 25-60°C.  $V_{oc}$  was observed to increase linearly with temperature and Eq. (2) was used to explain the temperature dependence of  $V_{oc}$ . The temperature dependence of  $V_{oc}$  has directly been correlated to the temperature dependence of quasi-Fermi levels of the polymer and the PCBM under illumination. Alternatively the temperature dependence of the  $V_{oc}$  in the present case has been attributed to the temperature dependence of built-in voltage ( $V_{bi}$ )<sup>16</sup>. The structure of an OPV device contains a thin active organic layer sandwiched between two metal electrodes. For the devices containing electrodes with different work-functions, in thermal equilibrium the Fermi level alignment takes place and an electric field is developed which is known as built-in electric field. The corresponding voltage between the two electrodes is known as the built-in voltage ( $V_{bi}$ ). The built-in electric field for electrons is directed from anode to cathode. Generally,  $V_{bi}$  is given by the difference of the work-function of the two electrodes ( $\Delta W$ ). But if electrodes make ohmic contact with the organic materials, an accumulation of charge carriers takes place in the vicinity of the electrodes and band bending takes place. Because of this band bending  $V_{bi}$  now becomes less than the  $\Delta W$ . As the temperature reduces  $V_{bi}$  increases and because of increment in  $V_{bi}$ ,  $V_{oc}$  increases<sup>18</sup>. The results of Eq. (2) are good enough for inorganic solar cells but their applicability to OPV devices is an open question, though they have been used to interpret  $V_{oc}$  in OPV devices<sup>18</sup>. Figure 5 shows

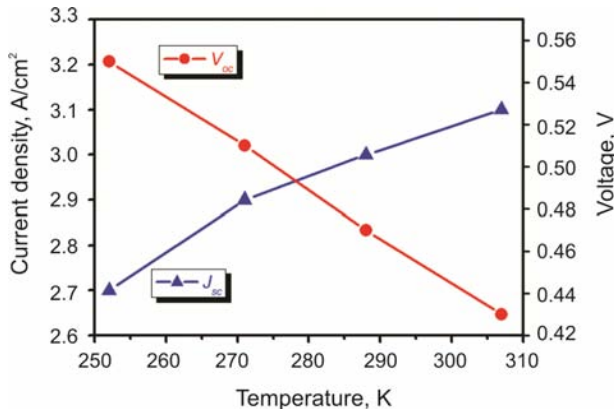


Fig. 4– Variation of  $V_{oc}$  and  $J_{sc}$  as a function of temperature

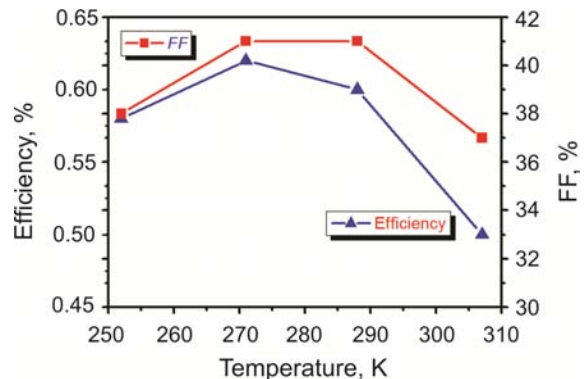


Fig. 5– Variation of  $FF$  and  $\eta$  of ITO/H<sub>2</sub>Pc(23 nm)/C<sub>60</sub> (40 nm)/Bphen(8 nm)/Al solar cell as a function temperature

the variation of  $FF$  and  $\eta$  of the  $H_2Pc$  based OPV device with temperature. The observed temperature dependence of  $FF$  is almost similar to that of  $J_{sc}$ .  $ZnPc$  based device also exhibit the similar behaviour (not shown). This behaviour can qualitatively be understood in terms of temperature dependent series resistance of the OPV devices.

### Conclusions

The thicknesses of OPV devices have been optimized to get the best performance. Temperature has been found to have a significant effect on device performance. The dark current under reverse bias and at low temperatures has been attributed to be governed by the tunneling of the charge carriers through large injection barriers. The overall efficiency of the device increases first and then decreases with reduction in temperatures.

### References

- Kim J Y, Lee K, Coates N E, Moses D, Nguyen T Q, Dante M & Heeger A J, *Science*, 317 (2007) 222.
- Hauch J A, Schilinsky P, Choulis S A, Childers R, Biele M & Brabec C J, *Solar Energy Mater Solar Cells*, 92 (2008) 727.
- Krebs F C & Spanggaard H, *Chem Mater*, 17 (2005) 5235.
- Lungenschmied C, Dennler G, Neugebauer H, Sariciftci S N, Glatthaar M, Meyer T & Meyer A, *Solar Energy Mater Solar Cells*, 91 (2007) 379.
- Noda T, Ogawa H & Shirota Y, *Adv Mater*, 11 (1999) 283.
- Kumar H, Kumar P, Bhardwaj R, Sharma G D, Chand S, Jain S C & Kumar V, *J Phys D: Appl Phys*, 42 (2009) 15103.
- Brabec C J, Cravino A, Meissner D, Sariciftci N S, Fromhertz T, Rispiens M T, Sanchez L & Hummelen J C, *Adv Funct Mater*, 11 (2001) 374.
- Mihailetchi V D, Blom P W M, Hummelen J C & Rispiens M T, *J Appl Phys*, 94 (2003) 6849.
- Mutolo K L, Mayo E I, Rand B P, Forrest S R & Thompson M E, *J Am Chem Soc*, 128 (2006) 8108.
- Lampert M A & Mark P, *Current Injection in Solids*, (Academic, New York), 1970.
- Kumar P, Jain S C, Kumar V, Misra A, Chand S & Kamalasanan M N, *Synth Met*, 157 (2007) 905;
- Kumar P, Misra A, Kamalasanan M N, Jain S C & Kumar V, *J Phys D:Appl Phys*, 40 (2007) 561.
- Kumar P, Chand S, Dwivedi S & Kamalasanan M N, *Appl Phys Lett*, 90 (2007) 23501
- Jain S C, Willander M & Kumar V, *Conducting Organic Materials and Devices* (Academic Press, San Diego), 2007.
- Schilinsky P, Waldauf C, Hauch J & Brabec C J, *J Appl Phys*, 95 (2004) 2816.
- Katz E A, Faiman D, Tuladhar S M, Kroon J M, Wienk M M, Fromherz T, Padinger F, Brabec C J & Sariciftci N S, *J Appl Phys*, 90 (2001) 5343.
- Peumans & Forrest S R, *Appl Phys Lett*, 79 (2001) 126.
- Kumar P, Jain S C, Kumar H, Chand S & Kumar V, *Appl Phys Lett*, 94 (2009) 183505.